23rd ABCM International Congress of Mechanical Engineering
December 6-11, 2015, Rio de Janeiro, RJ, Brazil

INFLUENCE OF EXPERIMENTAL CONFIGURATION ON THE ESTIMATION OF THE BIOT NUMBER IN A SIMPLE SETUP DESIGNED TO ESTIMATE THE THERMAL CONDUCTIVITY OF SOLID MATERIALS

L. L. Beretta
lucasberetta@id.uff.br
D. C. Moreira
dcmoreira@id.uff.br
L. A. Sphaier
lasphaier@id.uff.br
L. C. S. Nunes
luizcsn@id.uff.br

Laboratorio de Mecanica Teorica e Aplicada. Laboratorio de Opto-Mecanica. Departamento de Engenharia Mecanica (TEM-PGMEC). Universidade Federal Fluminense. Rua Passo da Patria, 156, Sao Domingos, Niteroi, RJ, Brazil.

Abstract. The main objective of this work is to analyze the influence of experimental setup configuration on estimation of the Biot number considering a simple experiment designed to estimate the thermal conductivity. A simple heat conduction fin model was fitted to the temperature fields acquired with an infrared camera. Based on that, the Biot number was estimated. The experiments were performed with two distinct experimental configurations. In the first configuration, only one surface was subjected to heat exchange by convection and radiation with the surroundings, while all other surfaces were thermally insulated. In the second configuration, the back side of the sample-holder was removed, keeping the top and below insulation, and it was assumed that the surfaces had the same convective and radiative losses on both symmetrical vertical faces. In both cases, the camera was positioned in horizontal direction. The distance between the camera and the sample was the same in all configurations. The experimental data acquired so far show good compatibility with theoretical predictions

Keywords: *thermography, biot number, fin model, temperature fields*

1. INTRODUCTION

The thermal conductivity is one of the most important thermophysical properties of materials. Experimentally, this property can be determined through a variety of methods. One example is the guarded heat flow meter (GHFM) method, which is based on the determination of the heat flux created by temperature difference between surfaces of the sample (Moreira *et al.*, 2011, 2012). The transient hot wire (THW) is another standard method that can be employed for assessing the thermal conductivity of a material. In this method, the temperature of a linear heat source, or hot wire, embedded in the analyzed material is measured and used to evaluate the thermal conductivity (Santos, 2005; Xie, 2006; Toberer, 2012). Infrared thermography can also be employed to estimate thermal conductivity. This is a powerful non-intrusive technique for assessing temperature fields from the infrared radiation of the sample surface (Cotta, 2009; Moreira *et al.*, 2013, 2014). The Infrared thermography is most commonly used for determining the thermal diffusivity of materials (Philippi *et al.*, 1995; Miettinen *et al.*, 2008; Laskar *et al.*, 2008).

A simple experimental arrangement using an infrared camera was developed to investigate the thermal conductivity augmentation in epoxy nanocomposites filled with metal oxides nanoparticles (Moreira *et al.*, 2013, 2014). In this experimental procedure, each tested specimen was allocated in a heat-insulating sample-holder. The specimen base was kept constant and one surface was exposed to the surrounding environment and its temperature fields were recorded, while all other surfaces were insulated. Using the same approach, the influence of the distance between infrared camera and specimen on the estimated Biot number was studied by Beretta *et al.* (2014). In this way, the main goal of this work is to use the same experimental setup, but now comparing the results obtained for specimens with only one surface exposed to the environment with those obtained in tests with two surfaces exposed to the surrounding environment. For this purpose, two materials with low thermal conductivity, polymethylmethacrylate (PMMA) and polytetrafluoroethylene (PTFE), were tested under these different conditions and the Biot number was estimated for each case. This parameter was determined using a classical fin model fitted to the measured temperature fields.

2. EXPERIMENTAL SETUP

The experimental apparatus consisted of an infrared camera, a thermal plate, a protective chamber and an adjustable sample holder. The infrared (IR) camera employed in the experiments was manufactured by FLIR, model A325 G, with a resolution of 320x240pixels, mounted with 1196960 lens, which has a focal length of 9.7mm and minimum working distance of 200 mm. The thermal plate was used as the heat source, and provided a constant heat flow to one end of the sample. The protective chamber is made of styrofoam with its inner side covered by black paper, and is responsible for isolating the experimental setup from external radiation and air flows. The sample holder was made of balsa wood and covered by black paint. During the experiments, the sample holder was positioned in a way that the camera was facing the front surface of the sample. Figure 1 shows the experimental setup with all its components.

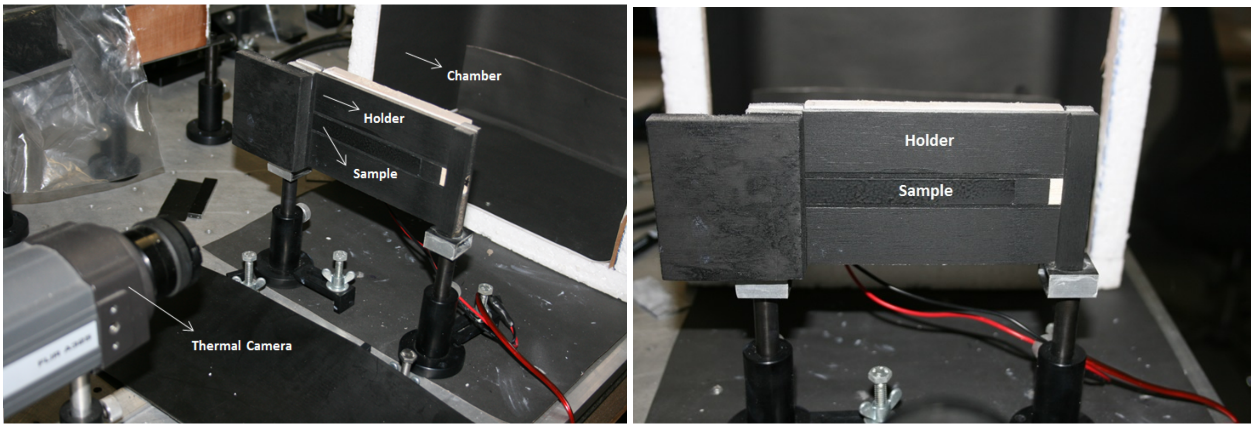

Figure 1. The experimental apparatus to estimate the thermal conductivity, and the sample holder with a specimen, all covered by black paint.

Two polymeric materials were tested in this study, Polymethylmetacrylate (PMMA) and Polytetrafluorethylene (PTFE). These materials were chosen for being homogeneous and isotropic. Samples of both materials were fabricated with dimensions of 100 mm $\times$ 13 mm $\times$ 5 mm. In order, to get an opaque surface with high and known emissivity, the samples were covered by black paint, as can be seen in Fig.1. A removable block on the back part of the sample holder enabled tests with only one surface of the sample exposed to the environment or with two surfaces exposed. In the first case, or case 1, only the front surface of the sample was exposed to the environment, while all other faces were insulated, except for the one where the heat source was applied. In the second analyzed case, or case 2, both the front and rear surfaces of the sample were exposed to the environment, while all other surfaces apart from the one where the heat source was applied were insulated. The temperature fields of the front surface in each configuration were acquired with the IR camera. Figure 2 depicts the cross-section of both experimental configurations.

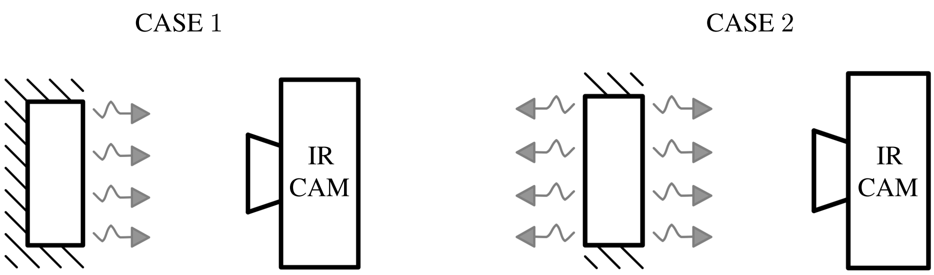

Figure 2. Illustration of both test cases, with only one side exposed to the environment (Case 1) and with both sides exposed (Case 2).

The temperature fields were all acquired at steady state, and the calculations were based on the average of 30 images. In addition, little temperature variation was observed in the vertical direction, such that the temperature fields were also averaged in this direction, and only the temperature variation in the horizontal direction was considered. The distance between the camera and the sample was 200 mm. It is worth mentioning that it is very important to define the sample's limits in the infrared image, so it is possible to correlate the sample length in milimeters with it's length in pixels.

2.1 Mathematical equations

A schematic diagram of the heat transfer problem in the proposed experiment is shown in Fig. 3. It is important to notice that the bar in the experimental apparatus is long enough, so the temperature at the tip is equal to the environment temperature, T_f. In addition, even though the thermal plate may offer a uniform heat flow at the base, instead of uniform temperature, both boundary conditions are valid at steady state. Since we measure the whole temperature field at the bar surface, a prescribed temperature boundary condition at the base was chosen, with $T = T_b$ at the base.

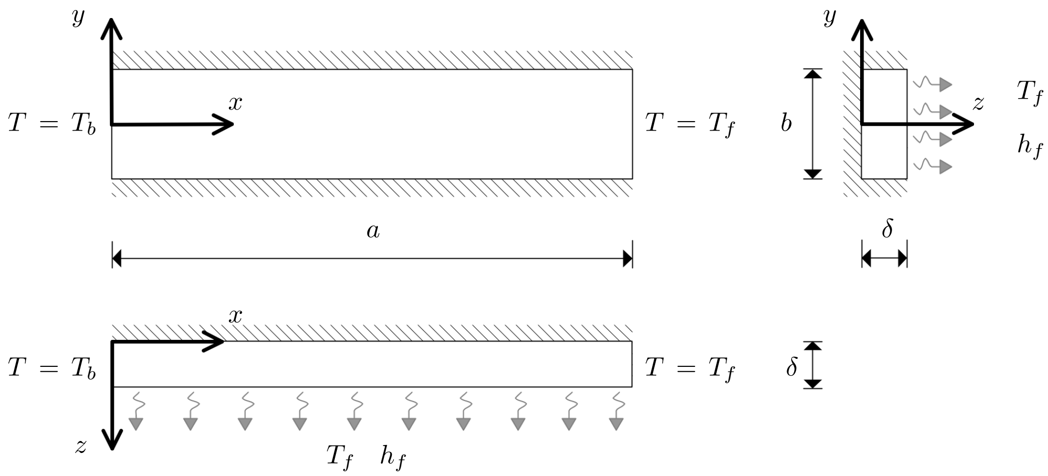

Figure 3. Schematic diagram of the heat transfer problem

Finally, it should be noted that the diagram exposed in Fig. 3 only shows the case where the back surface of the bar is insulated. Although it may seem that the configuration from Case 2, with two surfaces exposed to the environment, has been neglected in this representation, one should notice that Case 2 may also be described by this approach, due to symmetry condition. In this way, the only difference between the representation of both cases is the bar thickness, i.e., in Case 1, $\delta = c$, whereas in Case 2, $\delta = c/2$. Since we are considering that the thermal conductivity of the bar (k), the convective heat transfer coefficient (h_f), and the temperature at the base (T_b) are uniform, and both surfaces in y direction are insulated, it is possible to infer that there is no temperature variation in y direction. Also, if the bar is conductive or thin enough, the temperature dependence in z direction can also be neglected, and the heat transfer problem in this bar is simplified to a fin approach, where only the temperature variation in one direction is taken into account. This problem is described by the equations shown below:

$$\frac{d^2\theta}{d\xi^2} - m^2\theta = 0, \; for \;\; 0 \leq \xi \leq 1 \tag{1}$$

$$\theta = 1, \; at \, \xi = 0 \tag{2}$$

$$\theta = 0, \; at \, \xi = 1 \tag{3}$$

where,

$$m^2 = \frac{Bi}{\gamma^2} \tag{4}$$

$$Bi = \frac{h_f \, \delta}{k} \tag{5}$$

$$\gamma = \frac{\delta}{a} \tag{6}$$

and the dimensionless variables ξ and θ are defined by:

$$\xi = \frac{x}{a}, \qquad \theta = \frac{T - T_\infty}{T_b - T_\infty}. \tag{7}$$

Again, this equations are suitable for both cases, but the characteristic length (δ) must be changed accordingly:

$$\delta_1 = c, \qquad \delta_2 = \frac{c}{2}, \tag{8}$$

for Case 1 and Case 2, respectively. The solution to the system of equations (1), (2), and (3) is given by:

$$\theta(\xi) = \frac{\cosh(m\,(1-\xi))}{\cosh(m)}, \tag{9}$$

and the solution for $T(\xi)$ is found by substituting Eq. (9) into:

$$T(\xi) = (T_b - T_\infty)\theta(\xi) + T_\infty. \tag{10}$$

Equation (10) was fitted to the experimental steady state temperature distribution through the estimation of T_b, T_f, and Bi. The estimates for T_b and T_f were in agreement with experimental observations. It is important to remark that the classical fin approach neglects temperature variation along the sample cross-section, so it is valid for Bi < 0.1.

3. RESULTS

Figure 4 shows the temperature field of the PTFE specimen allocated in the sample-holder, which was obtained with the infrared camera. A similar result was observed with the PMMA specimen. The region of interest is marked with a blue box, and it was chosen to investigate the temperature distribution on the specimen surface along the horizontal coordinate. Initial and final horizontal positions of the specimen, which are associated with base and fluid temperatures, were carefully selected to ensure a suitable measurement. According to the temperature field of the specimen and sample-holder, it is possible to observe that the chosen boundary conditions are satisfactory.

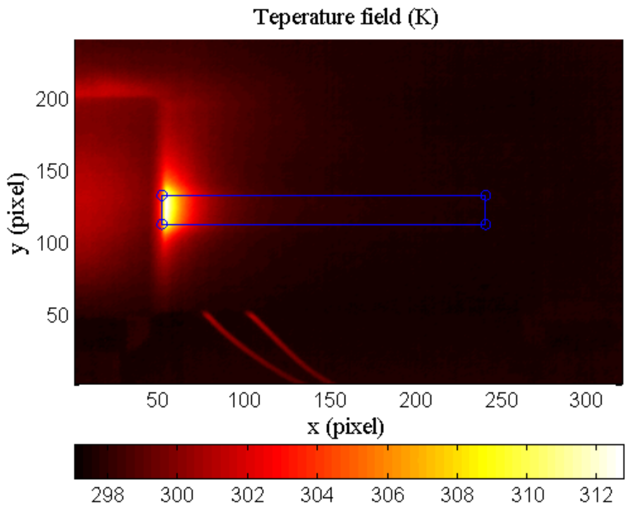

Figure 4. Temperature field.

Assuming that the temperature variation in the vertical direction of the region of interest is insignificant, the vertical average fin surface temperature distribution was evaluated. The mean values of temperature as a function of normalized horizontal coordinate for PMMA and PTFE specimens are illustrated in Fig 5. In this figure, the results for both experimental configurations, i.e., with one and two sides of fin free, together with curve fitting are also shown. As can be seen in these figures, the difference between fitted classical model and measured temperature is larger for one side free than for two sides free, mainly near base. These results were observed in all analyzed cases. It can indicate that the experimental configuration using two sides free is more appropriate.

Figure 6 shows the absolute error between experimental data and curve fitting for both experimental configurations, considering PMMA and PTFE specimens. These results were obtained from data presented in Fig 4. It can be noticed that the evaluated errors are relatively small; however, the values increase near the base. This discrepancy can be attributed to classical model that is not suitable to predict the temperature near the base. In all analyzed cases, the experimental-model errors for one free side were larger than for two sides free configuration.

To estimate the parameter m, Equation (10) was fitted to measured data, then the value of Bi for each configuration was calculated. Tables 1 and 2 present estimated values of m and Bi for PTFE and PMMA specimens considering both experimental configurations. Four tests were performed with the same samples to ensure repeatability of results. As can be seen from these results, values of ratio of m2 to m1 are approximately equal to $\sqrt{2}$. This value is in agreement with the classical fin model, considering that the convective heat transfer coefficient is the same for both configurations.

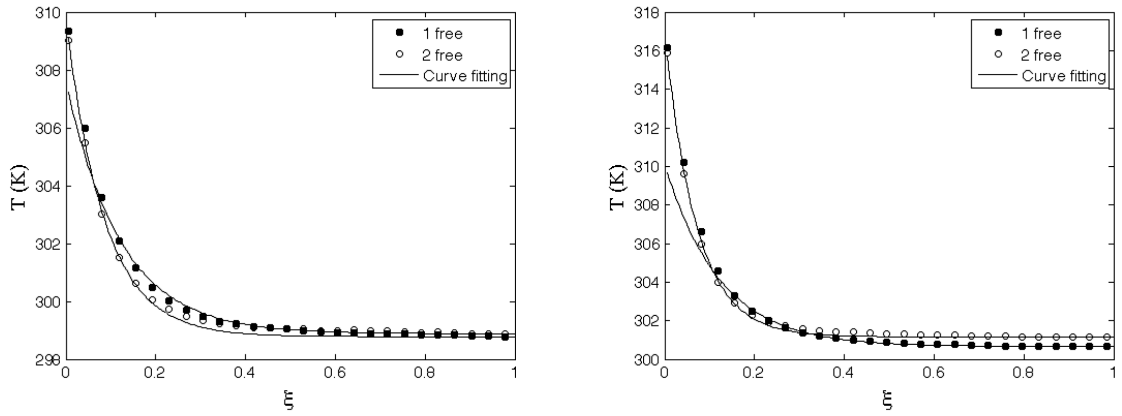

(a) PMMA (b) PTFE

Figure 5. Horizontal temperature distribution along PMMA and PTFE slabs for both experimental configurations.

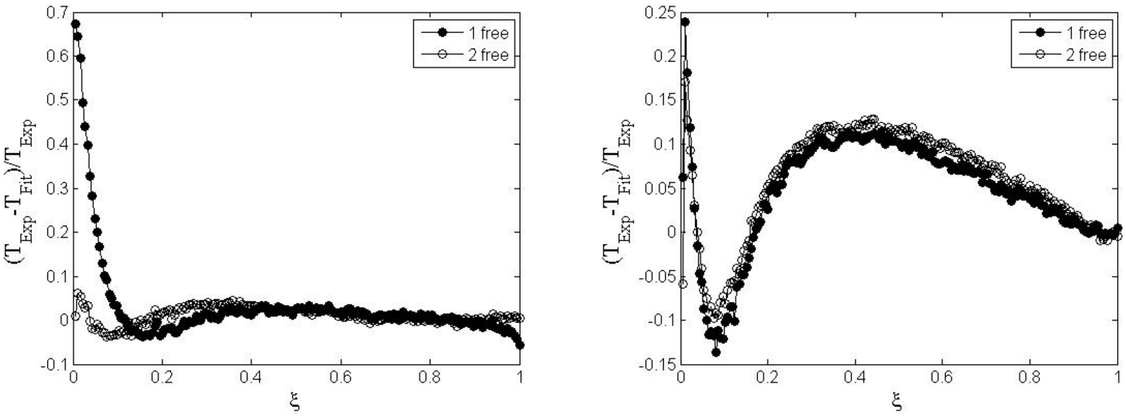

(a) PMMA (b) PTFE

Figure 6. Absolute error between experimental data and curve fitting for both cases.

Table 1. Estimated m and Bi values for the PTFE sample.

Tests	m_1	m_2	m_2/m_1	Bi_1	Bi_2
1	8.24	11.69	1.42	0.208	0.104
2	8.08	11.91	1.47	0.200	0.108
3	8.58	12.15	1.42	0.225	0.113
4	7.92	11.98	1.51	0.192	0.110

Table 2. Estimated m and Bi values for the PMMA sample.

Tests	m_1	m_2	m_2/m_1	Bi_1	Bi_2
1	11.08	14.01	1.26	0.285	0.116
2	10.91	13.28	1.22	0.277	0.102
3	7.91	11.01	1.39	0.145	0.070
4	8.23	14.27	1.73	0.157	0.118

4. CONCLUSIONS

In this work, a simple experiment for estimating the thermal conductivity of materials was analyzed. The proposed experimental methodology is based on a heat transfer fin model fitted to the surface temperature distribution in a bar, which is acquired by an infrared camera. Two polymeric materials were tested, Polymethylmetacrylate (PMMA) and Polytetrafluorethylene (PTFE), and two distinct experimental configurations were analyzed: only one surface exposed to the environment (Case 1), and two surfaces exposed to the surroundings (Case 2). In order to fit the model to the temperature distribution the Biot number, fluid temperature, and base temperature were estimated.

Both the fluid and base temperatures were in accordance with experimental observations. Also, no significant temperature variation in y direction was observed. The estimates for the Biot number were greater than 0.1 in all tests with the configuration of Case 1, and most of the Case 2 tests as well, showing that a more suitable model should be used, instead of the classical fin model, which is valid in cases where Bi < 0.1. The agreement between experimental data and fitted model was better when the configuration of Case 2 was used, and the estimates of Bi for this case were closer to 0.1, which indicates that this configuration is more appropriate than Case 1. The results showed a good repeatability, especially for tests with PTFE, and the ratio between Bi estimates of both experimental configurations was around 2, as expected. As a final comment, it should be remarked that this is a preliminary study and more tests should be carried out.

5. ACKNOWLEDGEMENTS

We would like to acknowledge the financial support given by FAPERJ, CNPq, CAPES, and Universidade Federal Fluminense.

6. REFERENCES

References

Beretta, L., Sphaier, L., Moreira, D.C. and Nunes, L., 2014. *Influence of Infrared Image Acquisition Distance on Parameter Estimation Using a Simple Heat Conduction Model*. 15th Brazilian Congress of Thermal Sciences and Engineering, November 10-13, 2014, Belém, PA, Brazil.

Cotta, C.P.N., 2009. *Problemas Inversos de Condução de Calor em meios Heterogêneos: Analise Teórico-Experimental via Transformação Integral, Inferência Bayesiana e Termografia por Infravermelho*. Master's thesis, UFRJ.

Laskar, J., B.S., Sardar, M., Jayakumar, T., P.J. and Raj, B., 2008. *Measurement of thermal diffusivity of solids using infrared thermography*. Materials Letters.

Miettinen, L., K.P., Merikoski, J., M.M. and Timonen, J., 2008. *In-plane thermal diffusivity measurement of thin samples using a transient fin model and infrared thermograph*. International Journal of Thermophysics.

Moreira, D.C., Sphaier, L.A., Reis, J.M.L. and Nunes, L.C.S., 2011. "Experimental investigation of heat conduction in polyester-Al2O3 and polyester-CuO nanocomposites". *Experimental Thermal and Fluid Science*, Vol. 35, pp. 1458–1462.

Moreira, D.C., Sphaier, L.A., Reis, J.M.L. and Nunes, L.C.S., 2012. "Experimental analysis of heat conduction in UPR-alumina nano-composites". *High Temperatures-High Pressures*, Vol. 41, pp. 185–195.

Moreira, D.C., Telles, M., Sphaier, L. and Nunes, L., 2013. "Enhanced lumped formulations for estimating the thermal properties of polymeric nanocomposites using infrared thermography". In *22th International Congress of Mechanical Engineering COBEM 2013.Ribeirão Preto, Brasil.*

Moreira, D.C., Telles, M., Sphaier, L. and Nunes, L., 2014. *Infrared thermography for estimating the thermal conductivity augmentation of polymeric nanocomposites*. High Temperatures-High Pressures.

Philippi, I., B.J., Maillet, D. and Degiovanni, A., 1995. *Measurement of thermal diffusivities through processing of infrared images*, Vol. 66. Review of scientific instruments.

Santos, W., 2005. *Aplicação da técnica de fio quente na determinação das propriedades térmicas de polímeros fundidos*, Vol. 15. Polímeros: Ciência e Tecnologia.

Toberer, E.S., B., 2012. *Advances in thermal conductivity*. Annual Review of Materials Research.

Xie, H., 2006. *Experimental analysis of heat conduction in upralumina nano-composites*, Vol. 17. High Temperatures-High Pressures.

7. RESPONSIBILITY NOTICE

The authors are the only responsible for the printed material included in this paper.